NeuroImage 244 (2021) 118616

Contents lists available at ScienceDirect

NeuroImage

journal homepage: www.elsevier.com/locate/neuroimage

Spectral signature of attentional reorienting in the human brain

Sara Spadone[a,*], Viviana Betti[b,c], Carlo Sestieri[a], Vittorio Pizzella[a], Maurizio Corbetta[d,e,f,1], Stefania Della Penna[a,1]

[a] Department of Neuroscience, Imaging and Clinical Sciences - and ITAB, Institute for Advanced Biomedical Technologies, G. d'Annunzio University of Chieti-Pescara, Italy
[b] Department of Psychology, Sapienza University of Rome, Italy
[c] IRCCS Fondazione Santa Lucia, Rome, Italy
[d] Department of Neuroscience, University of Padua, Italy
[e] Padova Neuroscience Center, University of Padua, Italy
[f] Departments of Neurology, Radiology, Neuroscience, Washington University St. Louis, USA

ARTICLE INFO

Keywords:
Attentional reorienting
Dorsal attention network
Beta rhythm
ERD/ERS
Magnetoencephalography
Visual network

ABSTRACT

As we move in the environment, attention shifts to novel objects of interest based on either their sensory salience or behavioral value (reorienting). This study measures with magnetoencephalography (MEG) different properties (amplitude, onset-to-peak duration) of event-related desynchronization/synchronization (ERD/ERS) of oscillatory activity during a visuospatial attention task designed to separate activity related to reorienting vs. maintaining attention to the same location, controlling for target detection and response processes. The oscillatory activity was measured both in fMRI-defined regions of interest (ROIs) of the dorsal attention (DAN) and visual (VIS) networks, previously defined as task-relevant in the same subjects, or whole-brain in a pre-defined set of cortical ROIs encompassing the main brain networks.

Reorienting attention (shift cues) as compared to maintaining attention (stay cues) produced a temporal sequence of ERD/ERS modulations at multiple frequencies in specific anatomical regions/networks. An early (~330 ms), stronger, transient theta ERS occurred in task-relevant (DAN, VIS) and control networks (VAN, CON, FPN), possibly reflecting an alert/reset signal in response to the cue. A more sustained, behaviorally relevant, low-beta band ERD peaking ~450 ms following shift cues (~410 for stay cues) localized in frontal and parietal regions of the DAN. This modulation is consistent with a control signal re-routing information across visual hemifields. Contralateral vs. ipsilateral shift cues produced in occipital visual regions a stronger, sustained alpha ERD (peak ~470 ms) and a longer, transient high beta/gamma ERS (peak ~490 ms) related to preparatory visual modulations in advance of target occurrence.

This is the first description of a cascade of oscillatory processes during attentional reorienting in specific anatomical regions and networks. Among these processes, a behaviorally relevant beta desynchronization in the FEF is likely associated with the control of attention shifts.

1. Introduction

The successful exploration of a visual scene requires a balance between boosting information processing at one location and shifting attention to other locations (Corbetta et al., 2002, 2008). Maintaining and shifting attention are fundamental control operations that depend on interacting cortical and subcortical circuitries (Fiebelkorn et al., 2018), whose underlying neural mechanisms are still poorly understood.

Two decades of functional MRI studies support the hypothesis that a dorsal frontoparietal attention network (DAN) exerts top-down modulation over the activity of visual (VIS) regions during stimulus- or goal-driven attentional *orienting*. i.e. when attention moves to a location or object of interest (Kastner et al., 1999; Hopfinger et al., 2000; Bressler et al., 2008; Spadone et al., 2015). Conversely, a ventral frontoparietal attention network (VAN) is jointly recruited with the DAN during *reorienting*, i.e. when attention shifts to a novel location of interest (Corbetta et al., 2008). Orienting and reorienting are spatially segregated in the DAN where medial parietal regions are involved in *shifting attention*, whereas lateral parietal regions are involved in *maintaining* attention to a relevant spatial location (Shulman et al., 2009; Capotosto et al., 2013).

While spatial patterns of task activation are suggestive of specific attention processes, the low temporal resolution of fMRI is not able to

* Corresponding author.
E-mail address: s.spadone@unich.it (S. Spadone).
[1] These authors contributed equally to this work.

https://doi.org/10.1016/j.neuroimage.2021.118616.
Received 23 March 2021; Received in revised form 20 July 2021; Accepted 22 September 2021
Available online 25 September 2021.
1053-8119/© 2021 Published by Elsevier Inc. This is an open access article under the CC BY-NC-ND license (http://creativecommons.org/licenses/by-nc-nd/4.0/)

describe the dynamics of human attention at high temporal resolution, which requires techniques like electroencephalography (EEG) or magnetoencephalography (MEG). However, these methods have been typically deployed by looking at the whole-brain level only at a subset of the relevant frequency-specific oscillations. The *orienting* of attention has been correlated with two main oscillatory mechanisms in parieto-occipital cortex (Jensen and Mazaheri, 2010; Gregoriou et al., 2015): a pre-stimulus event-related desynchronization (ERD) in alpha/beta (α/β) bands, a putative correlate of preparatory processes (Thut et al., 2006), and a post-stimulus event-related synchronization (ERS) in the gamma (γ) band, a putative correlate of top-down modulation of sensory information (Siegel et al., 2008; Bauer et al., 2014). Even fewer studies have investigated oscillatory activity during *reorienting* (Sauseng et al., 2005; Daitch et al., 2013; Proskovec et al., 2018). This behavior has been associated with a delayed alpha (and beta) band ERD in posterior regions (Sauseng et al., 2005; Proskovec et al., 2018), and a more widespread increase of power in the theta band (Proskovec et al., 2018). Theta synchronization during reorienting is also supported in both DAN and VAN regions by electrocorticographic (ECoG) recordings from human subjects monitored intracranially for epilepsy (Daitch et al., 2013).

Importantly, from a psychological and task analysis standpoint, the reorienting response involves multiple processes. For instance, in the classic Posner paradigm (Sauseng et al., 2005; Daitch et al., 2013; Proskovec et al., 2018), the reorienting response, triggered by the presentation of targets at unattended locations, includes additional processes such as the violation of expectancy (invalid targets are necessarily less frequent than valid targets), target detection, and motor preparation/response. The co-occurrence of multiple cognitive operations confounds the specificity with which attention processes can be localized.

To summarize: different studies point to alpha and beta desynchronization in posterior regions during orienting/reorienting of attention, and a separate theta synchronization for reorienting. However, the waveform parameters (amplitude, latency, onset-to-peak duration) underlying pure reorienting responses and their behavioral relevance have never been jointly investigated. Moreover, no study to date examined these mechanisms vis-à-vis the extant fMRI literature.

Our study presents three important innovations as compared to the extant literature. First, our continuous attention paradigm (Shulman et al., 2009) isolates attention processes (maintaining/reorienting) from target- and response-related activity (Capotosto et al., 2013, 2015; Spadone et al., 2015). Second, our high temporal resolution MEG data were obtained from fMRI-defined attention-specific regions, as well as at the whole-brain level. This strategy links electrophysiological mechanisms to fMRI networks with high precision. Thirdly, we analyzed, as a trial unfolds, the time course of multiple frequency-specific modulations linking significant electrophysiological modulations to behavioral performance.

We test specific hypotheses based on our model of attention (Corbetta et al., 2008), and previous electrophysiological results (Sauseng et al., 2005; Daitch et al., 2013; Proskovec et al., 2018). In general, we predict that different reorienting-related processes shall unfold concurrently in time, even within the same network or region. Specifically, based on the joint role of the DAN and VAN in reorienting and related theta-specific synchronization (Daitch et al., 2013), we predict an increase of oscillatory power at lower frequencies in the early phases of re-orienting. This signal may correspond to the postulated 'circuit-breaker' or 'network' reset signal interrupting the current attention state (Corbetta et al., 2008). As the focus of attention moves and begins to engage a new location, the fMRI studies indicate the recruitment of fronto-parietal regions of the DAN. Specifically, the frontal eye field (FEF) is one of the core regions given the link between overt (oculomotor) and covert attention signals (Rizzolatti et al., 1987; Corbetta, 1998). Based on animal (Buschman and Miller, 2007) and human studies (Sauseng et al., 2005; Siegel et al., 2008; Jensen and Mazaheri, 2010; Proskovec et al., 2018) we predict prominent beta (possibly alpha) modulations tracking the movement (shift) of attention. Finally, the engagement of the DAN leads to the development of top-down>bottom-up interactions with visual cortical regions for selection of attended stimuli and filtering of unattended stimuli (Bressler et al., 2008; Spadone et al., 2015; Meehan et al., 2017). This sensory-driven attentional modulation shall correspond to asymmetric modulations of α and γ activity in the contralateral visual cortex (Fries et al., 2001; Siegel et al., 2008; Jensen and Mazaheri, 2010).

2. Materials and methods

2.1. Continuous attention paradigm

Stimuli were generated using the MATLAB Psychtoolbox-3 and consisted of two drifting Gabor patches constantly presented on the left and right locations over a light gray background, with the following parameters: 2 cycles/° spatial frequency, 0.7 °/s drift rate, 3° diameter, 5.5° eccentricity from central fixation. Participants were instructed to maintain fixation on a central cross while covertly directing attention to one of the two patches. The to-be-attended location was indicated by the appearance of a cue consisting of a 300 ms isoluminant change in the patch color after which the stimulus turned gray. During the cue period, both patches were colored (pink, cyan) but only one color was relevant for cueing (e.g. pink) that was shown at the beginning of both task runs and counterbalanced across runs. If the relevant color appeared in the same location compared to the previous one, the attention had to be maintained (stay cue) in that location. If, however, the relevant color appeared in the opposite location, attention had to be shifted (shift cue) to the new location (Fig. 1A). This paradigm was chosen to exploit the benefit of exogenous cueing, which allows investigating maintenance vs. shifting of attention while reducing a strong contralateral sensory response triggered by the presentation of a single peripheral cue. Cue location correctly predicted with 80% probability the location of targets, consisting of a 150 ms change in the orientation of one patch (clockwise/anticlockwise), but did not predict when the target would appear. After each cue, either zero, one, or two targets could be presented, encouraging subjects to continuously attend to the cued location. Targets could not occur earlier than 1 s after a cue, to provide enough time for post-cue (e.g., ERD/ERS) analyses, and cues could not occur earlier than 2 s after a target, to provide enough time for a motor response. Subjects were instructed to detect and discriminate orientation changes as fast as possible by pressing a right/left button on a response box with their right hand. Targets occurred on average every 11 s and cues appeared at random intervals between 4 and 6 s. These parameters, used to generate two pseudorandom sequences of stimuli, were the same as our previous EEG-TMS studies (Capotosto et al., 2013, 2015). Finally, each of the two pseudorandom stimulus sequences was designed using three blocks of attention task (each lasting 300 s) interleaved by a 15 s period of fixation, which was used to minimize fatigue and drop of attention. The stimulus sequence also included a 30 s period of fixation at the beginning of the run.

2.2. Subject selection and study protocols

Subject enrollment was based on a preliminary behavioral session aimed at measuring task performance and monitoring eye position during task execution with an infrared eye-tracking system (Iscan etl-400, RK-826 PCI). Only subjects showing a significant validity effect (valid>invalid) on target discrimination accuracy and able to maintain central fixation after both stay and shift cues were enrolled in the study (details can be found in Spadone et al. 2015; SI Materials and Methods). After the selection procedure, a total of 20 right-handed (Edinburgh Inventory) healthy volunteers with no previous psychiatric or neurological history participated in the MEG study after providing written informed consent according to the Code of Ethics of the World Medical Association and to the Ethics Committee at the University of Chieti. From this

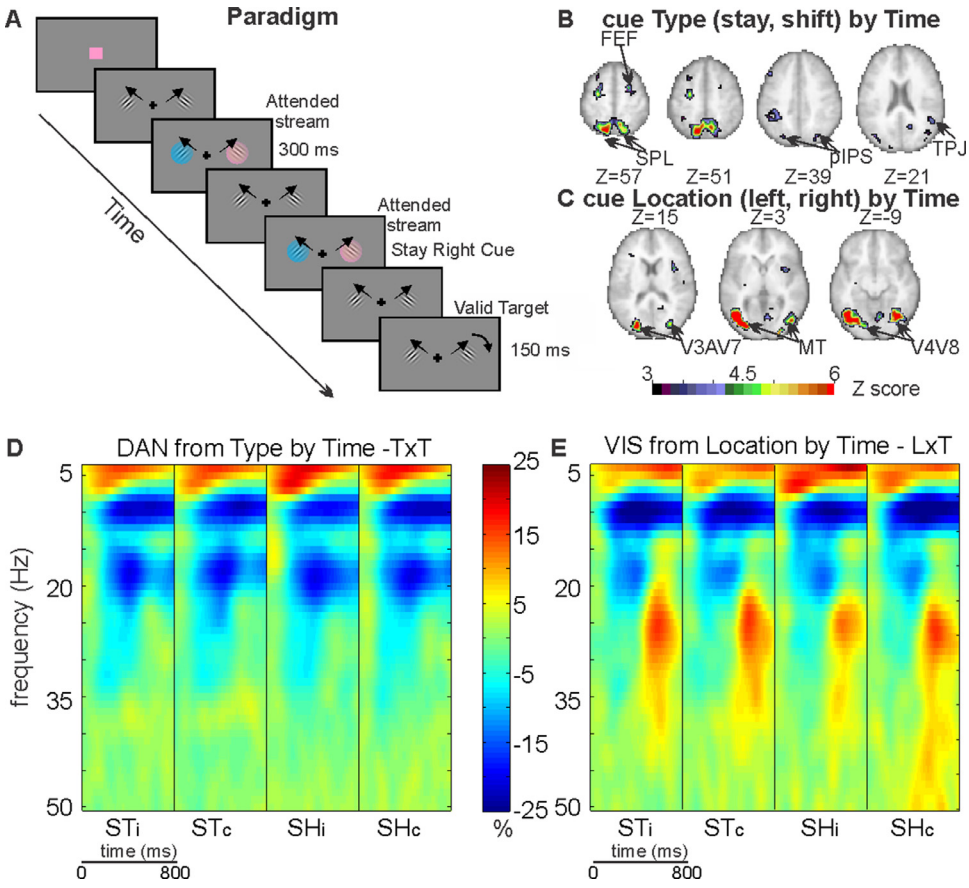

Fig. 1. Paradigm, ROIs and ERD/ERSgrams. (A) Example of the display sequence in the visuospatial attention task. (B) Voxelwise map of the contrast between BOLD activity for shift vs. stay cues (reorienting effect) that isolated DAN TxT regions together with the right TPJ in the VAN. (C) Voxelwise map of the contrast between activity for left vs. right cues (contralateral effect) that isolated VIS LxT regions. (D-E) Group average time-frequency plots during the post-cue period for the two sets of ROIs (DAN TxT, D, and VIS LxT, E), separately for the four possible cue conditions [ipsilateral stay (STi), contralateral stay (STc), ipsilateral shift (SHi) and contralateral shift (SHc) to the ROI].

sample 2 subjects were excluded in the preprocessing step; thus the following analyses are related to 18 subjects (age range = 19–28 y old; 13 females). The same subjects also participated in our previous fMRI study (Spadone et al., 2015). The original sample size of the fMRI study consisted of 21 subjects, but 1 subject was excluded due to the incompatibility of the head size with the MEG helmet. Subjects underwent a MEG session including 3 resting state (fixation) runs lasting 5 min each, followed by two runs of the visuospatial attention task, each lasting about 16 min. The visuospatial attention task lasted for ~32 min (16 min × 2 runs). The order of the two task runs was counterbalanced across subjects. In this work, we present only results on the visuospatial attention task.

2.3. MEG recordings and eye movement monitoring

MEG signals were recorded by the multi-channel MEG system installed at the University of Chieti and consisting of 153 dc-SQUID integrated magnetometers (Della Penna et al., 2000; Pizzella et al., 2001). Magnetic fields were continuously acquired at a 1025 Hz sampling rate while participants performed the resting state and the visuospatial attention sessions. The magnetic signals were simultaneously recorded with two orthogonal electrocardiographic and two orthogonal electrooculographic (EOG) channels that were used for offline artifact rejection and to monitor horizontal eye movements. The head position relative to the MEG sensors was detected after each run by five coils placed on the scalp, whose positions were digitized together with anatomical landmarks. Moreover, to provide the anatomical reference to build the volume conductor for MEG data analysis, each subject underwent a high-resolution structural image using a sagittal M-PRAGE T1-weighted sequence (TR=8.14 ms, TE=3.7 ms, flip angle=8°, voxel size=1 × 1 × 1 mm^3). During the recordings participants were comfortably seated and watched the stimuli presented via an LCD projector placed outside the magnetically shielded room, projecting images on a pair of 45° mirrors and a translucent screen positioned inside the shielded room in front of the subject. Subjects responded using a LUMINA LU400 Response Pad (Cedrus Corporation).

2.4. Behavioral data and eye movement analysis during MEG experiment

During the MEG experiment, we further verified that subjects maintained the same capacity to carry out the task as in the preliminary behavioral session selecting the experimental group, by evaluating the presence of a validity effect and the continuous maintenance of central fixation. Specifically, we performed paired t-tests over subjects to compare reaction times and discrimination accuracy between valid and invalid targets. Moreover, we analyzed the event-related time courses of horizontal eye position time-locked to the presentation of cues. To this aim, EOG signals were converted in degrees of visual angle using the calibration factor obtained from calibration runs recorded at the beginning and the end of each visuospatial attention run. To improve the SNR in the EOG signals, we removed the high-frequency noise and the baseline drift from the horizontal and vertical signals. We removed the first noise source through the application of a median filter. For the latter noise source, we applied a multilevel 1-D wavelet decomposition at level nine using Daubechies wavelets (Bulling et al., 2011). The reconstructed decomposition coefficients, providing a baseline drift estimation, were subtracted from the original signals, considerably reducing the drift offset. Moreover, intervals across eye-blinks were removed from the horizontal EOG. To this aim, we first identified the eye-blinks peaks on the vertical EOG, through statistical analysis (mean+2std), and the blink duration across these peaks through the analysis of the signal derivative. Then, the residual drift was reduced detrending the signals over 4 s epochs following each cue, corresponding to the minimum inter-cue interval. The horizontal eye position time courses, locked to the

presentation of cues, were estimated in the same interval used to analyze source activities (0–800 ms post-cue interval). Finally, the ability to maintain central fixation during the MEG experiment was quantified for each experimental condition through one-sample t-tests against 0 (no deviation) on the mean values estimated over the post-cue interval.

2.5. Data preprocessing and ROI selection

The quality of MEG signals was inspected to remove time epochs with excessive noise (Larson-Prior et al., 2013). Two subjects were excluded from further analyses in the preprocessing step, due to abnormal artifacts and technical problems. Then, MEG signals were analyzed by applying the pipeline based on independent components analysis (ICA) (Mantini et al., 2011; Spadone et al., 2012) that separates artifactual from brain-related independent components (IC). For each IC, the sensor map was projected in the source space using a weighted minimum-norm least squares (WMNLS) approach implemented in Curry 6.0 (Compumedics Neuroscan, El Paso, TX, USA). This step was performed using the co-registered individual anatomical images to obtain a realistic head model sampled through 4 mm side isotropic voxels. The individual source maps were then normalized to the Montreal Neurological Institute brain template (MNI 152). Finally, voxel-level vector activities were obtained from each region of interest by linearly combining the non-artifactual IC time courses weighted by the related source map values [as in Sebastiani et al. 2014]. Specifically, the source-space signals were computed for voxels corresponding to the centroids of two sets of regions of interest (ROIs), selected on the same subjects from the evoked response during cue in our previous fMRI study (Spadone et al., 2015). This selection was obtained through a voxel-wise ANOVA with Cue Type (stay, shift), Cue Location (left, right), and Time (MR frames) as factors. The Cue Type by Time interaction map identified regions that exhibited a shift-related (shift>stay) modulation, regardless of cue location. Specifically, a strong shift-related response was identified in core regions of the dorsal attention network (DAN from the Cue Type by Time contrast map - TxT, Figs. 1B, S1): the superior parietal lobule (SPL), the dorsal aspect of the human frontal eye fields (dFEF) and the posterior intraparietal sulcus (pIPS). A significant response occurred also in the right TPJ, a core region of the VAN, as predicted by the model (Corbetta et al., 2008).

The Cue Location by Time interaction map identified regions that responded in a spatially selective manner independent of cue type (contralateral>ipsilateral) in occipital regions of the visual network (VIS from Cue Location by Time contrast map - LxT, Figs. 1C, S1): the ventral (corresponding to visual V4–V8), dorsal (corresponding to V3a–V7), and lateral occipital regions (corresponding to the human middle temporal visual area, MT). When associating fMRI ROI with MEG source positions, spheres with a radius of a few mm (compatible with our voxel size – 4 mm) and centered in the centroid of the fMRI ROI can be used. This represents a compromise accounting for the different spatial resolution of the two techniques and the inherent source displacement in fMRI, which is related to vascular and not electrophysiological sources. Using the MEG voxel activities with the closest positions to the centroid of the fMRI ROIs is consistent with previous works associating MEG activity to fMRI ROIs (Torquati et al., 2005; Favaretto et al., 2021).

In summary, these fMRI analyses identify two sets of regions: “control” regions of the DAN/VAN involved in orienting/reorienting, irrespective of hemifield, and sensory processing regions of the visual system showing a hemifield-specific visual modulation.

2.6. Time-frequency analysis

We ran time-frequency analyses on cue epochs, from −500 ms to 1250 ms after the trigger, to investigate the effect of maintaining and shifting visuospatial attention across hemifields on MEG rhythms. First, cue trials including time epochs removed during the quality check were rejected. Following this step, given an ROI centroid, an average number of 88(± 2) cues per condition (i.e. ipsilateral stay, contralateral stay, ipsilateral shift, contralateral shift to the ROI centroid) was available for the spectral analysis. Before running the time-frequency analysis, for each cue type and each orthogonal direction of the vector activity, the average event-related activity phase-locked to the cue onset was removed to extract the non-phase-locked rhythms. The removal was performed applying a standard procedure based on an adaptive algorithm using orthogonal projections (Della Penna et al., 2004). This method assumes invariance of the shape but not of the amplitude of the evoked response across trials. Thus, the trial-averaged evoked response to cues is adaptively regressed out from each trial. Next, the time-frequency representations (TFRs, which are time courses of the power spectrum density) were estimated using the Morlet wavelets for each trial, activity direction, ROI centroid, and subject. The frequency and temporal bins were 1 Hz and 1 ms respectively. Since we were interested in analyzing rhythm modulations in a large range of frequencies (4:50 Hz), the width of the wavelet expressed in number of cycles was not fixed but varied as a linear function of frequency, according to:

$$\text{width} = 7 + \frac{\text{frequency} - 10}{4} \tag{2}$$

These parameters were selected to set the width at about 7 in the alpha band, as this value corresponds to a good balance between temporal and frequency resolutions (Jensen et al., 2002; Spadone et al., 2020) and to extend this balance to the whole frequency interval. To obtain the total TFR for each ROI centroid, the TFRs were summed across the three directions of vector activity and averaged across trials involving homologous cues. For all the total TFRs, we computed the event-related desynchronization/synchronization (ERD/ERS) as a function of frequency and time as instantaneous percentage power variations after cues (E) compared to the mean power in a baseline period (R) of 300 ms prior the presentation of cues, according to $\text{ERD/ERS}(t,f)(\%) = \frac{E(t,f)-R(f)}{R(f)} * 100$. We show ERD/ERSgrams averaged across subjects (Fig. 1D, E).

Finally, for each physiological frequency band, we identified the individual most reactive frequency (i.e. the frequency bin with the largest ERD/ERS peak) and we analyzed the individual onset, latencies, and amplitudes of ERD/ERS peaks to investigate the effect of attention conditions on the dynamics of rhythm modulations. The frequency boundaries defining the physiological bands, chosen according to the EEG/MEG literature (Neuper and Pfurtscheller, 2001), were: θ = 4:8 Hz; α = 8:15 Hz; low-β=15:26 Hz; high-β/γ = 20:50 Hz. Of note, the β (usually showing ERD after spatial cues) and γ (showing ERS) bands partially overlap since the typical range of these bands was expanded to account for individual variability of the most reactive frequency across all the ROI centroids and subjects. An automatic procedure searched for the temporal and spectral position of the maximum ERD/ERS within a band. The interval for searching ERD/ERS peaks was (90,+800 ms) after cue onsets. We excluded the last part of the trial intervals as they could be contaminated by target occurrence (target could not occur before to 1 s after a cue and the cue-target interval was on average 2.1 s). Moreover, the time interval used to estimate the TFRs was larger than the one used for the analysis of power modulations, to avoid contamination of the wavelet edge effect. When inspecting the individual total TFRs, we noticed that multiple power peaks and troughs could appear at a given frequency band, corresponding to multiple ERD/ERS peaks. In some cases, due to a lower SNR, the amplitude of the multiple peaks could differ only slightly, making it difficult to identify the real latency of the ERD/ERS. Due to this variability, a valid ERD/ERS peak could also occur before the one selected by the automatic procedure. We thus introduced an adaptive threshold for each frequency band, above which the procedure searched for the first local peak, which could also not correspond to the absolute minimum/maximum:

$$\text{THR} = \left(1 - \frac{\text{relERD/ERS}}{100}\right) \cdot |\text{ABS\_M}| \tag{3}$$

where ABS_M represents the absolute minimum/maximum amplitude of the ERD/ERS at the corresponding frequency band and relERD/ERS

represents the relative error of ERD/ERS. To estimate this error, we used the propagation of the relative errors of E and R on the ERD/ERS formula. Notably, both these relative errors were assumed to be the same and were computed as the relative errors on the total TFR estimate (relE=relR). We thus estimate the relative error in the baseline epoch (relR), where no effects of the task should affect the mean power density which should be assumed constant. Specifically, relR was the ratio between the standard deviation across trials in the baseline epoch and the R in the ERD/ERS formula. For all the extracted peaks, at the ERD/ERS responsive frequency, we also detected the onset of desynchronization/synchronization, as the last zero-crossing before reaching the ERD/ERS peak, and we computed the onset-to-peak duration as the difference between peak latency and onset. Finally, we computed the network average value as the average of ERD/ERS properties across ROIs centroids belonging to each functional network (DAN from TxT, VIS from LxT).

2.7. Statistical analysis

We run the statistical analysis on the ERD/ERS properties averaged over ROI centroids belonging to each network [DAN from TxT and VIS from LxT (Spadone et al., 2015)]. We tested the effect of the specific experimental condition (stay ipsilateral, stay contralateral, shift ipsilateral, shift contralateral to ROI) on ERD/ERS properties [onset, peak amplitude, and latency, and ERD/ERS onset-to-peak duration (peak latency minus onset)] for each frequency band. Specifically, we used repeated-measures ANOVAs with the network (DAN, VIS), cue Type (Stay, Shift), and Cue Side (ipsilateral or contralateral to ROI) as factors. We looked for differences of ERD/ERS peak amplitude as they can be associated with increased or reduced involvement in a condition compared to the others, and for differences of ERD/ERS latency and of onset-to-peak duration as a measure of processing time. Finally, we analyzed the temporal sequence of the obtained rhythm modulations in the different frequency bands. To this aim, one-way ANOVAs with frequency band as a factor (θ, α, low-β, high-β/γ) were computed on ERD/ERS onset-to-peak duration and peak latency during shifts of attention. Of note, before comparing these parameters, we rescaled the ERD/ERS onset-to-peak duration of each frequency band to the corresponding wavelet duration, to consider the different spread due to the variable wavelet duration across frequencies. Furthermore, since different wavelet durations could also affect the comparison of ERD/ERS properties within a particularly wideband (e.g., gamma), we demonstrated the absence of a systematic switch of the responsive frequencies across cueing conditions within each frequency band using three-way ANOVAs with network (DAN, VIS), Cue Type (Stay, Shift) and Cue Side (ipsilateral or contralateral to ROI) as factors (all $ps > 0.05$).

2.8. Brain-behavior analyses

To assess the behavioral significance of the oscillatory modulations specifically associated with the control of attentional reorienting in the DAN, we tested whether the parameters describing the power modulations involving the Cue Type factor (i.e. ERD onset-to-peak duration in the β band) were associated with the subsequent target performance. First, we estimated the Pearson correlation ($p < 0.05$) between modulations of ERD/ERS properties in response to shift versus stay cues (i.e. shift-stay ERD onset-to-peak duration of DAN ROIs in the β band) and target discrimination accuracy (shift vs. stay cues) across subjects. Then, we performed a brain-behavior analysis focused on the modulation of β oscillations following shift cues and preceding valid targets observed in the FEF. At the individual level, we separated shift trials into two groups according to target discrimination reaction times (RTs) using a median split (slower vs. faster discrimination). We then estimated the ERD parameters in the beta band from the FEF for slow and fast trials and we tested the significance of their difference through a paired *t*-test across subjects.

2.9. Control analysis on spatial specificity of frequency-specific modulations

To test the spatial distribution and specificity of reorienting-related modulations, an extended whole-brain analysis using a large set of ROI centroids was conducted separately for each band. ROIs were selected from a previously published set of 169 ROIs (Baldassarre et al., 2014) removing the sub-cortical regions and obtaining 158 ROIs. These represent the nodes of nine well characterized resting-state networks: Dorsal-Attention (DAN), Ventral Attention (VAN), Somatomotor (SMN), Visual (VIS), Auditory (AN), Language (LAN), Default Mode (DMN), FrontoParietal (FPN), Control (CO). The fMRI-defined ROIs used in the main analysis (DAN from TxT and VIS from LxT) replaced the corresponding ROIs in this extended set. For each ROI centroid, we evaluated the effect of reorienting on ERD/ERS parameters that were significantly modulated in the main analysis (i.e., peak amplitude for theta and alpha band, the onset-to-peak duration for beta and low-gamma band). To avoid the inclusion of possible random effects due to noise, we thresholded the ERD/ERS using individually estimated errors on the TFR (as relERD/ERS in Eq. (3)). For all the regions, paired t-tests were applied over subjects to compare ERD/ERS parameters across conditions ($p < 0.05$). For each frequency band of interest, the group average differences between relevant conditions of ERD/ERS parameters (e.g. shift vs. stay, or contralateral vs. ipsilateral cues) were displayed over the set of ROI centroids using a network visualization tool (BrainNet Viewer Xia et al. 2013). Region centroids were represented as spheres on the lateral and dorsal views of an MNI brain. Different colors represented increases or decreases of ERD/ERS parameters between conditions whereas different sizes represented significant and not significant differences between conditions. Furthermore, for each frequency band, we show the bar plot illustrating the mean of the ERD/ERS parameters across the nodes belonging to each functional network. For all the networks, paired t-tests were conducted over subjects to compare ERD/ERS parameters across conditions ($p < 0.05$).

3. Results

3.1. Behavioral data and eye movement results during MEG experiment

Paired t-tests were conducted over subjects to compare reaction times and discrimination accuracy between valid and invalid targets. As expected, subjects were more rapid ($p = 2 \bullet 10^{-5}$) and accurate ($p = 3 \bullet 10^{-4}$) to discriminate targets at the attended vs. unattended locations, an indication of a positive modulation by spatial attention on performance. Subjects could maintain central fixation during the MEG experiment. Specifically, mean values across subjects after the baseline period were $0.01^{\circ} \pm 0.03^{\circ}$ (mean±standard error) and $0.00^{\circ} \pm 0.03^{\circ}$ for right and left stay cues and $0.01^{\circ} \pm 0.04^{\circ}$ and $0.01^{\circ} \pm 0.03^{\circ}$ for right and left shift cues (where negative numbers refer to a leftward movement). Importantly, one-sample t-tests against 0 (no deviation) on the mean values estimated over 800 ms post-cue showed no significant deviation from the fixation cross for each experimental condition (all ps>0.05).

3.2. MEG results

We measured multiple frequency-specific modulations of event-related desynchronization/synchronization (ERD/ERS) induced by different cueing conditions (ipsilateral stay, contralateral stay, ipsilateral shift, contralateral shift to the ROI) in the DAN and VIS network. Fig. 1D, E show DAN (VIS) ERD/ERS 2D plots obtained from averaging signals across ROI centroids defined in specific fMRI contrast maps on the same subjects (Spadone et al., 2015): for the DAN, cue Type by Time (TxT) (Figs. 1B, S1), and the VIS, cue Location by Time (LxT) (Figs. 1C, S1).

Both DAN and VIS showed a power increase in the θ [4–8 Hz] band (~30%, group average of ERS peak), a decrease in the α [8–15 Hz] (~40%, group average of ERD peak) and low-β [15–26 Hz] (~30%)

bands, and an increase in the high-β/γ [20–50 Hz] (~30%). In the VIS regions this high-β/γ power increase was even stronger (~40%).

Next, to isolate modulations related to attentional processes, we evaluated differences in ERD/ERS properties [onset, peak amplitude, and latency, and ERD/ERS onset-to-peak duration (peak latency minus onset)] across cueing conditions using separate repeated-measures ANOVAs, with Network (DAN, VIS), Cue Type (Stay, Shift) and Cue Side (contralateral, ipsilateral to ROI) on each ERD/ERS parameter and frequency band. Given our interest in the reorienting response, only the main effect of Cue Type and its interaction with other factors will be presented. For each frequency band, we show the significant effects through (i) violin plots, to represent the distribution of individual values of ERD/ERS properties extracted from single ROI centroids and averaged across ROIs belonging to each functional network; and (ii) group-averaged waveforms of power modulations, used for graphical purposes since the results of our statistical analyses were based on individual data. Since the analysis of peak latency and onset-to-peak duration yielded similar results, we only report the results of the analysis of ERD/ERS onset-to-peak duration. We found frequency-specific modulations of ERD/ERS properties that were common, but also highly spatially specific in the two networks, and that overlapped in time after the onset of the cue, as described below.

To test that the results reported at the ROI level were indeed specific at the whole-brain level, ERD/ERS modulation were also measured in a larger set of fMRI-defined ROIs covering the whole brain and multiple networks (DAN, VAN, SMN, VIS, AN, LAN, DMN, FPN, CO).

Herein, we first discuss the major frequency-specific modulations, then their temporal sequence during a trial ("different rhythm modulations at different times during reorienting").

3.3. Low-β ERD/ERS modulations in the DAN during shifts of attention

The group average time-frequency ERD/ERS maps revealed a clear desynchronization after cue onset in the low-β band (15 ÷ 26 Hz), which was stronger in Cue Type x Time DAN ROIs as compared to Location x Time VIS ROIs (Figs. 1D, E, 2B). The ERD peaked at about 400 ms and remained sustained till 800 ms post-cue onset. The response in visual regions was more transient (Fig. 2B). Notably, β ERD lasted longer for shift as compared to stay cues. This difference was quantified using a three-way ANOVA, which revealed a significant Network by Cue type interaction ($F_{1,17}$=4.9, $p < 0.05$) on ERD onset-to-peak duration. Importantly, longer ERD following shift as compared to stay cues occurred specifically in DAN regions (Duncan post-hoc results, $p < 0.05$, Fig. 2A, B). Similar effects were found for ERD latency. No significant differences were found on ERD peak amplitude ($F_{1,17}$=2.3, $p > 0.05$) or ERD onset ($F_{1,17}$=0.003, $p > 0.05$). The sustained β ERD shift-related modulation in the DAN is shown for one representative subject (Fig. S2) and averaged across subjects (Fig. 2B).

We used a within-subject classification approach to test the possibility to predict the cue type (stay or shift) from the duration of the low-beta ERD. Specifically, we extracted the onset-to-peak duration from low-beta ERD time courses, computed using blocks of twenty trials, and randomly selected 100 blocks for each subject. The parameters extracted from the blocks were used as input for the classification analysis. A linear support vector machine (SVM) was trained on 75% of the randomly selected blocks and tested on the remaining blocks. The procedure was repeated 1000 times and the average classification accuracy was computed for each subject. The average value across subjects was about 62% and significantly higher compared to the classification accuracy computed on the random assignment of the cue type ($p < 1 \bullet 10^{-5}$). This finding demonstrates that is possible to predict the locus of attention based on the temporal parameter of the beta oscillations. In summary, regions of the DAN showing a stronger response for shift than stay cues in fMRI also show a more sustained β ERD modulation.

To verify that these ROI-driven analyses were not spatially biased, the analysis was repeated on 158 ROIs from nine resting-state networks: DAN, VAN, SMN, VIS, AN, LAN, DMN, FPN, and CO. Significant differences in β ERD onset-to-peak duration for shift vs. stay cues ($p < 0.05$, larger spheres in Fig. 2D) were localized in dorsal prefrontal and posterior parietal regions of the DAN, specifically the fMRI localized FEF ROI, adjacent dorsal precentral cortex, and an intraparietal region, close yet not identical to the fMRI localized IPS ROI. When the analysis was repeated by averaging ROI-specific signals over networks (Fig. 2C) no significant effects remained (all ps>0.05), supporting the idea that β ERD during reorienting was highly localized to some DAN regions, specifically the FEF.

Since the dorsal precentral regions showing a shift>stay β ERD modulation overlapped with the motor cortical region activated by the key press to the target, we ran a control analysis to rule out the possibility that such desynchronization was related to motor preparation (Pfurtscheller, 1981). Accordingly, we selected the region of the motor cortex ($x = -38$ $y = -31$ $z = 57$, anterior 2.2 cm from the dorsal precentral region) exhibiting the strongest target-related response in our previous fMRI study (Spadone et al., 2015). The two-way ANOVAs with Cue Type and Cue Side as factors revealed no significant differences between stay and shift cues in both ERD parameters, amplitude ($F_{1,17}$=0.60, $p > 0.05$) and onset-to-peak duration ($F_{1,17}$=0.30, $p > 0.05$). This control, therefore, rules out a motor preparation explanation of our results.

Next, we tested whether the shift-related sustained β ERD modulation in FEF was reliable at the level of individual subjects. To answer this issue, β ERD onset-to-peak duration was extracted from single trials or from ERD time courses averaged over blocks of trials of different numerosity (10, 15, 20 trials). For each subject and block numerosity, 100 trial blocks were randomly selected and used to test the significance of the differences (shift vs. stay) through paired t-tests. The increase of onset-to-peak duration was significant in 14 out/18 subjects using at least 15 trials to estimate the time-frequency ERD/ERS responses and the corresponding parameters. An individual ERD onset-to-peak duration for stay and shift cues averaged over blocks of 15 trials is shown in Fig. S3. At the single-trial level, the β ERD modulation reached statistical significance in half of the subjects.

Finally, we examined the behavioral relevance of β ERD modulations. Across subjects sustained β ERD for shift vs. stay correlated with target discrimination accuracy ($r = 0.70$, $p < 0.005$, Bonferroni corrected, scatterplot Fig. 3A). Thus, subjects with more prolonged shift-stay β ERD in the DAN were more accurate in discriminating targets following shift than stay cues. Moreover, we performed a brain-behavior analysis focused on the modulation of beta oscillation in the FEF following shift cues and preceding valid targets. This analysis showed a significant difference between the latency of the ERD peak between shift trials followed by slower vs. faster target discrimination (see individual reaction times in Fig. 3B, divided into slow -red- and fast -blue- ones according to the individual median split; the corresponding ERD latencies are compared in Fig. 3C). Given that the ERD onset did not differ between the two groups of shift trials, we associated the slower ERD with prolonged processing. Specifically, more prolonged ERD in the beta band corresponded to faster target discrimination and vice-versa.

In summary, spatial reorienting of attention (shift>stay cues) increased the onset-to-peak duration of low-β ERD in regions of the DAN, especially FEF. This result is robust both at the whole-brain and at the single-subject level. This modulation is also behaviorally relevant as a more prolonged β de-synchronization was associated with better and faster visual discrimination.

3.4. Distributed low-frequency modulations following reorienting cues

A more widespread modulation occurred across multiple regions and networks when comparing signals for shift vs. stay cues. This modulation was a shorter latency (peak ~330 ms) ERS in the θ band across regions of the DAN (TxT) and VIS (LxT)(Fig. 1D, E). This θ synchronization was stronger for shift than stay cues as quantified using a three-way ANOVA

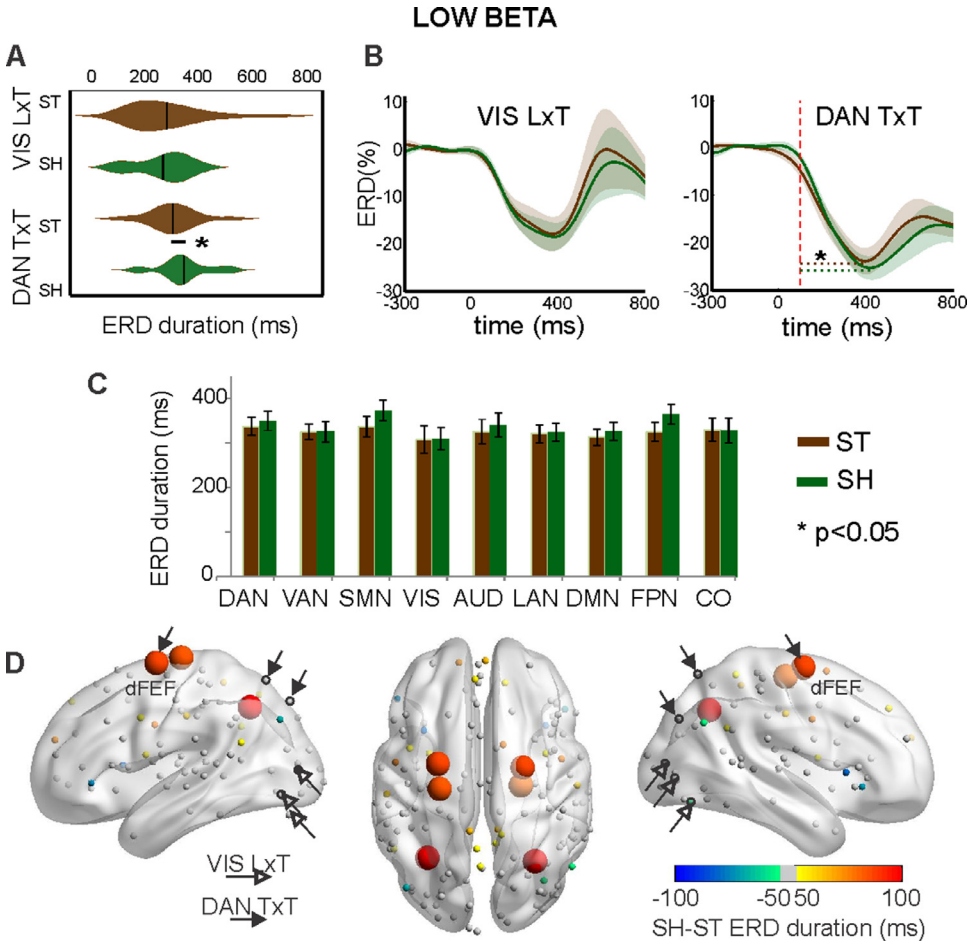

Fig. 2. DAN selective BETA power modulations. (A-B) A priori analysis on DAN TxT and VIS LxT. (A) Violin plots showing the distribution of ERD onset-to-peak duration in the β band. The significant Network by Cue Type interaction is marked with and asterisk ($p < 0.05$). (B) Graphical (but not statistical) representation of the effects found in the β band. We here show the group average waveform of the power modulations in the β band following stay (ST) and shift (SH) cues at the responsive frequency averaged across regions belonging to VIS LxT and DAN TxT, where error ranges represent standard error. The Red line marks the group average onset of ERD. Notably, the ERD/ERS parameters were estimated for each ROI centroid and subject, then averaged across networks. (C-D) Whole-brain analysis. Bar plot showing network averaged β ERD onset-to-peak duration following stay and shift cues (C) and their differences in the extended set of ROIs represented by spheres on a standard brain in lateral and dorsal views. The color of the sphere indicates the difference and the size indicates the significant (large) and not significant (small) difference. Our a priori defined regions are highlighted with a black arrow (DAN TxT with full arrows, VIS LxT with empty arrows) (D).

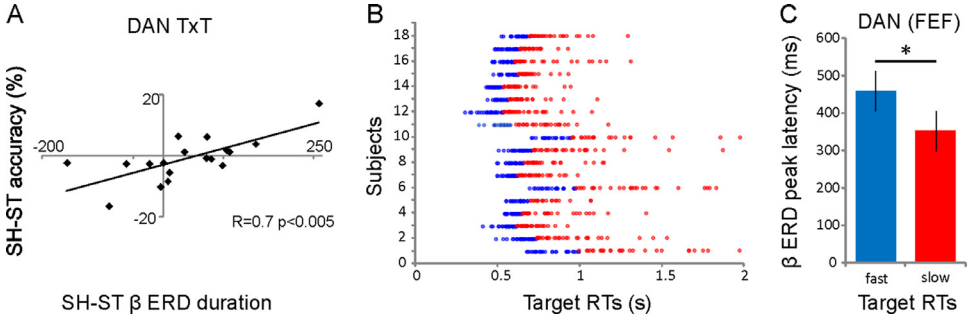

Fig. 3. Brain-behavior relationship. (A) Plot showing the significant relationship between the reorienting effect (shift vs. stay) observed in the β ERD onset-to-peak duration and target discrimination accuracy.(B) Scatter plot of the individual reaction times; the blue and red colors are respectively assigned to RTs below and above the individual median split. (C) Comparison between β ERD peak latencies for fast and slow valid target discrimination following shift cues ($p < 0.05$).

on the ERS peak amplitude. There was a significant main effect of Cue Type (θ: $F_{1,17}$=5.1, $p < 0.05$) across both DAN and VIS networks (Fig. 4A, B). No other interaction effect involving Cue Type was found in the θ band. The whole-brain analysis indicated that this early θ ERS involved multiple regions ($p < 0.05$, Fig. 4D using spheres with larger size) across multiple networks ($p < 0.05$, Fig. 4C). They include the temporo-parietal junction (right>left), inferior insula, frontal operculum and anterior cingulate that correspond to VAN, FPN, and CO networks. These regions and networks belong to the right dominant ventral attention network and bilateral control networks that are modulated in fMRI by reorienting, task initiation, and task offset (Dosenbach et al., 2007; Seeley et al., 2007; Corbetta et al., 2008).

3.5. *VIS-specific modulations in α and γ bands during shifts of attention*

In the visual cortex, two main modulations were observed following the onset of the cue: a sustained ERD in the α band (Fig. 5) and a transient high β/γ band ERS (Fig. 6). These modulations were localized in LxT VIS ROIs (Fig. 1E). In the α band, the three-way ANOVA on the ERD amplitude revealed a significant three-way interaction ($F_{1,17}$=11.0, $p < 0.005$), indicating a stronger ERD for contralateral shift cues as compared to both ipsilateral shift ($p < 0.05$) and contralateral stay ($p < 0.005$) cues only in VIS regions (Fig. 5A). Interestingly, the ERD amplitude was also greater for ipsilateral compared to contralateral stay cues ($p < 0.05$). No effects involving Cue Type were found on ERD onset-to-peak duration (all p-values>0.05).

These effects indicate that the α band ERD is hemifield specific and occurs predominantly in visual occipital regions. The ERD amplitude modulates following a shift in the hemifield-specific allocation of attention (contra shift>ipsi shift and contra stay). These modulations are consistent with the classic α band ERD previously described (e.g., Sauseng et al. 2005, Thut et al. 2006, see discussion).

The high-β/γ band ERS was transient and late in the delay after the cue (Fig. 6). The three-way ANOVA on ERS onset-to-peak dura-

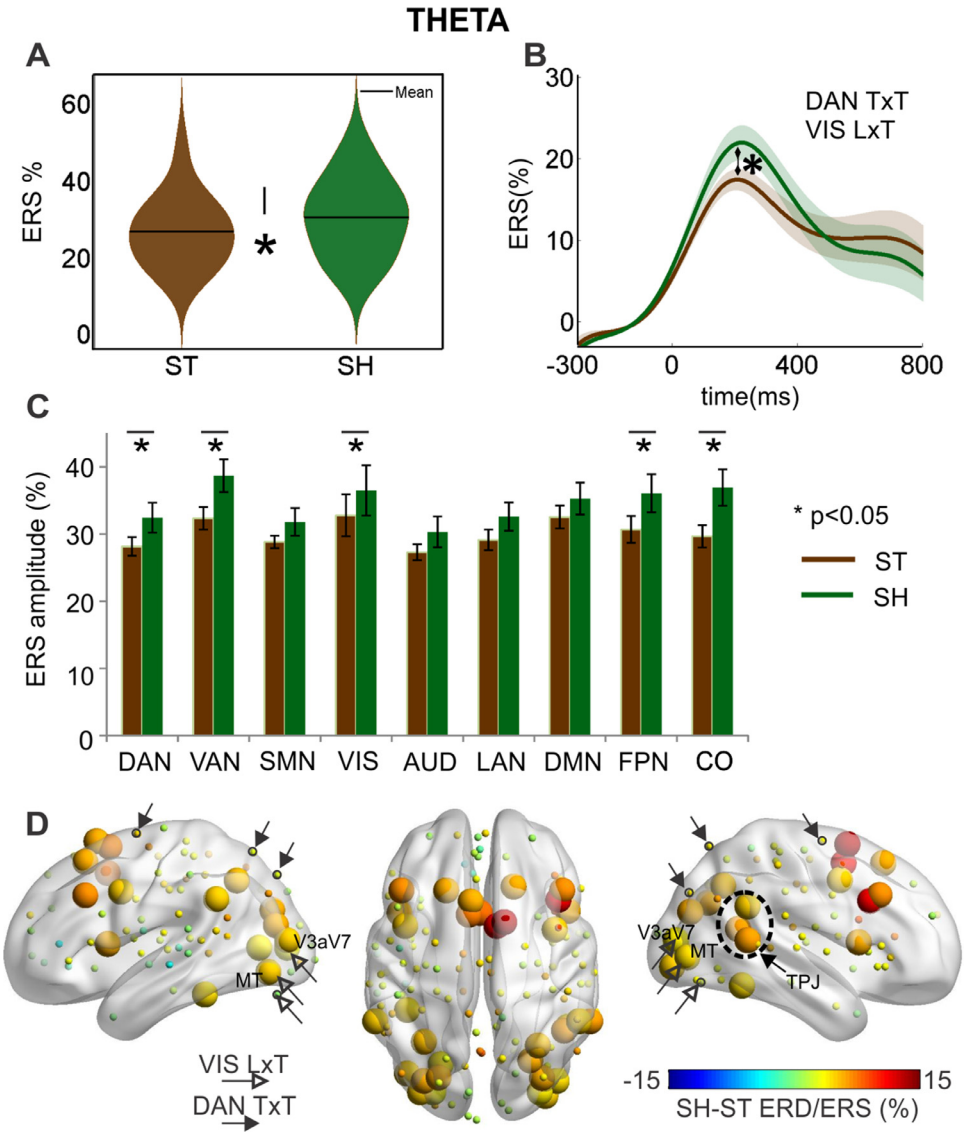

Fig. 4. Network and spatially unselective THETA power modulations. (A, B) A priori analysis on DAN TxT and VIS LxT. (A) Violin plots showing ERS peak amplitude in θ band following stay (ST) and shift (SH) cues and the significant main effect of cue type. (B) Group average waveforms of the power modulations following stay and shift cues at the responsive frequency averaged across networks. (C-D) Whole-brain analysis. (C) Bar plot showing network averaged ERS peak amplitude where the significant ($p < 0.05$) differences between shift and stay cues are indicated with asterisks. (D) Differences in θ ERS peak amplitude between shift and stay cues in the extended set of ROIs represented by spheres on a standard brain in lateral and dorsal views.

tion showed a significant three-way interaction ($F_{1,17}$=5.0, $p < 0.05$), explained by longer ERS for contralateral versus ipsilateral shift cues ($p < 0.05$) only in VIS regions (Fig. 6A). No significant effects were found on ERS amplitude ($F_{1,17}$=0.3, $p > 0.05$) or onset ($F_{1,17}$=0.2, $p > 0.05$). The whole-brain analysis localizes this modulation specifically to lateral visual occipital cortex near/at the middle temporal area (MT) contralaterally to the field of attention, especially for shift cues (Figs. 6C, D). The whole-brain network analysis confirms the localization to the visual network for both α band and high-β/γ band modulations (Figs. 5C, D, 6C, D).

In summary, spatially selective modulations of occipital regions include a sustained α desynchronization, concurrent with the β band desynchronization of control fronto-parietal regions, and a late transient high-frequency high-β/γ synchronization contralateral to the shift of attention. Since the cue consisted of a color change occuring both ipsilaterally and contralaterally, this high-frequency modulation is consistent with a boost of sensory processing at the new attended location in advance of the target, rather than a mere sensory response to the shifting cue.

3.6. *Different rhythms at different times during reorienting*

The separate frequency-specific modulations described above were all triggered by the presentation of a visual peripheral cue (a color change) instructing the observer either to stay on the same stream of visual stimuli or shift to the contralateral stream. The operation of shifting attention was behaviorally "covert", as indexed by the stability of eye movements, but produced a cascade of concurrent oscillatory effects that engaged different parts of the brain at different latencies, and with different time courses. Fig. 7 shows a qualitative scheme of these different oscillatory modulations displayed using the whole-brain analysis.

The presentation of the cue triggers a widespread theta synchronization at around 330 ms that involves both visual and dorsal attention regions, but also regions that belong to the ventral attention, frontoparietal, and cingulo-opercular networks. Around 400–450 ms, regions of the DAN (FEF, IPS) manifest a beta desynchronization that is longer when attention shifts. The degree of desynchronization is behaviorally relevant as it is associated with target discrimination performance. Nearly concurrently, occipital regions begin to desynchronize in the alpha band. Finally, the occipital cortex contralateral to an attention shift shows a focal high beta/gamma enhancement at around 500 ms post-cue. This response is not due to the presentation of a target but reflects enhancement for the attended stream of stimuli.

To quantitatively test this sequence, we compared ERD/ERS onset-to-peak duration and peak latency during shifts of attention between different bands through one-way ANOVAs with frequency (θ, α, low-β, high-β/γ) as the within-subject factor. This analysis was run on the fMRI localized ROIs of the DAN and VIS networks. Of note, the differ-

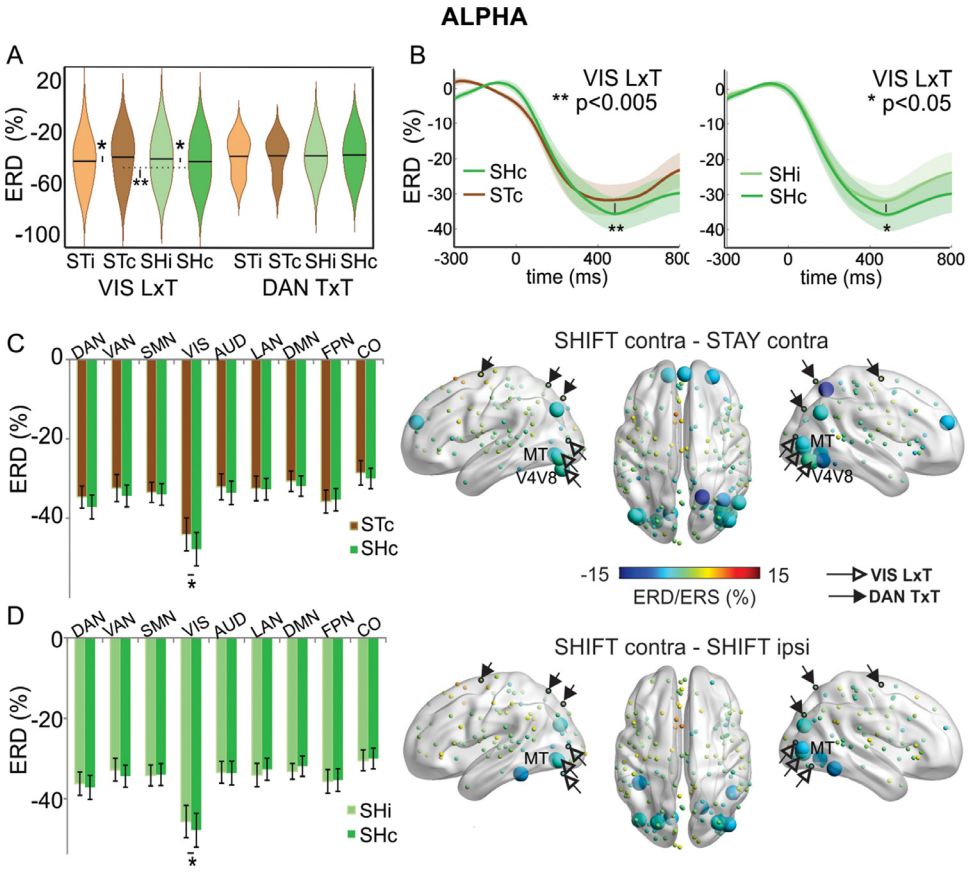

Fig. 5. VIS selective ALPHA power modulations. (A, B) A priori analysis on DAN TxT and VIS LxT. (A) Violin plots showing the significant Network by Cue Type by Cue Side interaction on ERD peak amplitude in the α band. (B) Group average waveforms of the power modulations in the α band following contralateral stay and contralateral shift cues (left graph) and following contralateral and ipsilateral shift cues (right graph) at the responsive frequency for VIS LxT. (C, D) Whole-brain analysis. (C) Bar plot showing network averaged α ERD peak amplitude following contralateral shift and contralateral stay cues and their differences in the extended set of ROIs. (D) Bar plot showing network averaged α ERD peak amplitude following contralateral and ipsilateral shift cues and their differences in the extended set of ROIs.

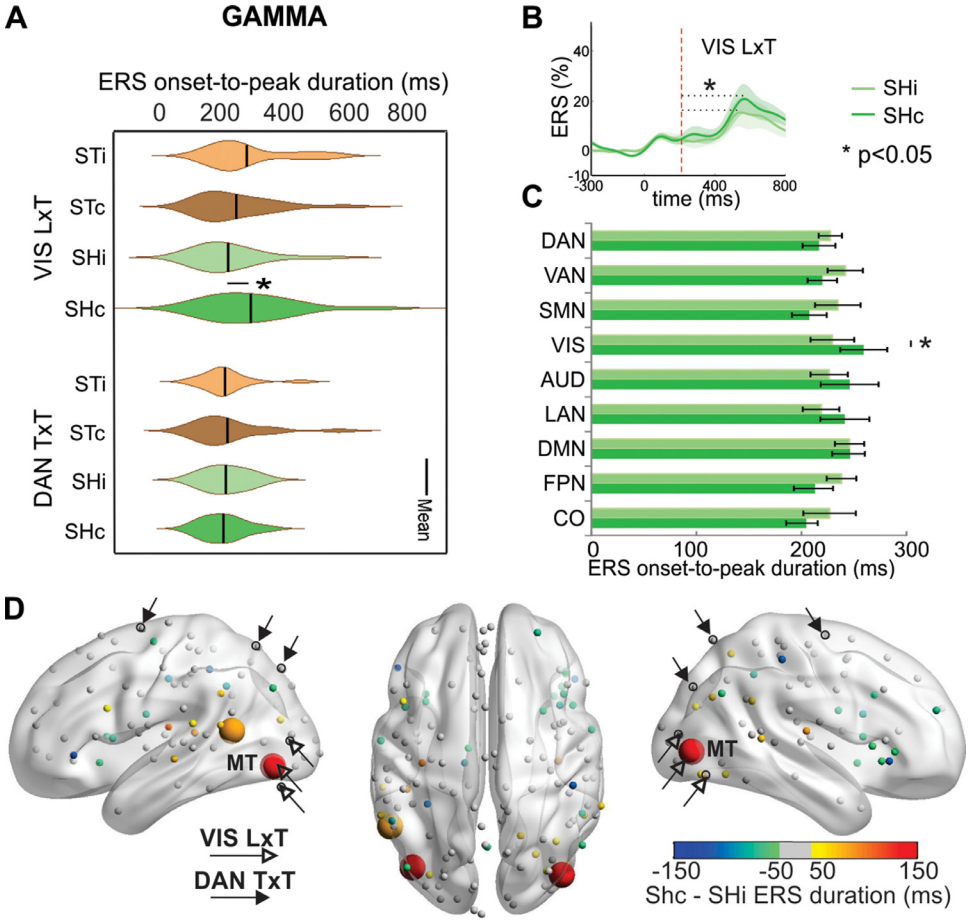

Fig. 6. VIS selective HIGH-BETA/GAMMA power modulations. (A, B) A priori analysis on DAN TxT and VIS LxT. (A) Violin plots showing the significant Network by Cue Type by Cue Side interaction on ERS onset-to-peak duration in the high-β/γ band. (B) Group average waveforms of the power modulations in the high-β/γ band following contralateral and ipsilateral shift cues at the responsive frequency for VIS LxT. (C, D) Whole-brain analysis. Bar plot showing network averaged high-β/γ ERS onset-to-peak duration following contralateral and ipsilateral shift cues (C) and their differences in the extended set of ROIs (D).

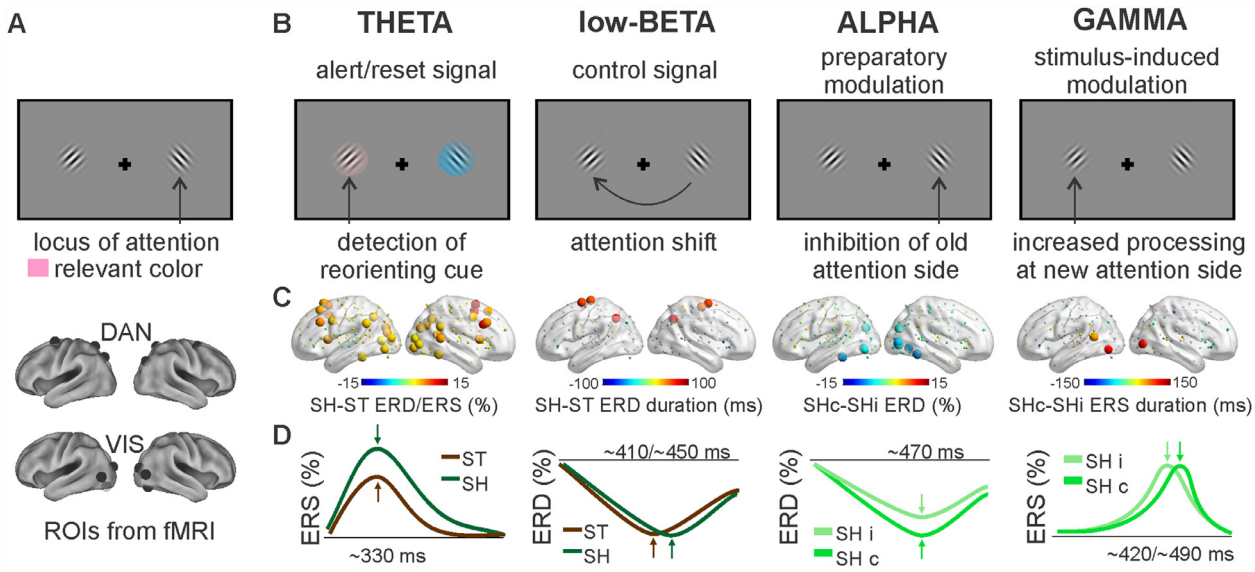

Fig. 7. Summary of significant shift-related power modulations in DAN TxT and VIS LxT regions. The sequence of different processes involved in the reorienting of attention to the contralateral hemifield and the associated rhythm modulations in DAN TxT regions and the VIS LxT. (A, B) Representation of the attentional processes involved in the reorienting response. (C) Modulated networks are indicated by blue (ERD) and red (ERS) spheres on an inflated brain representation. (D) Significant effects on ERD/ERS properties (*i.e.* onset, peak amplitude, and onset-to-peak duration) are represented as schematic waveforms.

ent temporal spread of the oscillatory modulations across frequencies, due to the variable wavelet duration, was considered by rescaling the ERD/ERS onset-to-peak duration of each frequency band to the corresponding wavelet duration.

The results of the ANOVA revealed significant differences between frequency bands for both the peak latency ($F_{3,51}$=4.5, $p < 0.01$) and onset-to-peak duration ($F_{3,51}$=7.4, $p < 0.0001$) of ERD/ERS. Post hoc tests showed that peak latency of θ ERS occurred before that measured in other bands (all ps<0.05), supporting the involvement of θ rhythm as an early alert/resetting signal. Moreover, power modulations of α and low-β bands, observed respectively in VIS and DAN regions, peaked at around the same latency (all p-values> 0.05), but were more sustained (longer onset-to-peak duration, all ps< 0.05), compared to those observed for high-β/γ in VIS regions. These temporal properties further support the hypothesis that the prolonged shift-related desynchronization of the β band represents the spectral signature of the control signal in DAN regions during reorienting. In contrast, the spatially selective modulations of ERD/ERS parameters observed in VIS regions could reflect the preparatory (α) and the stimulus-induced boosting (high-β/γ) of the sensory processing at the new cued location.

4. Discussion

In this study, we combined MEG recordings, a continuous attention paradigm not confounded by target- and response-related processes, and both fMRI localized ROIs in the DAN and VIS network, as well as whole-brain analysis across nine different brain networks, to identify oscillatory mechanisms associated with the visual reorienting response in the human brain. Consistently with previous studies (Sauseng et al., 2005; Proskovec et al., 2018), we confirm that the reorienting response is associated with multiple frequency-specific modulations of oscillatory activity that unfold concurrently in time across the brain.

We further highlight several novel results. First, by using strong fMRI spatial priors built on previous studies (Shulman et al., 2009, 2010; Spadone et al., 2015), our study allowed a clear association between brain regions/networks and modulations of oscillatory activity, confirmed by whole-brain analyses. We found a θ rhythm synchronization occurring in multiple control networks which is consistent with a reset signal triggered by the detection of a behaviorally relevant event that requires a change of the task set. Moreover, thanks to our pure reorienting paradigm, we clearly distinguished between reorienting-related modulations in α, low-β, and high-β/γ bands that are often confounded both in terms of their anatomical system and relevant attention process. Notably, within this cascade of oscillatory responses, we demonstrated the behavioral significance of the prolonged β desynchronization in the DAN, and especially in the FEF, which likely reflects control signals involved in re-routing information processing across hemifields.

4.1. β band suppression and the control of visuospatial attention

The DAN is recruited when observers direct their spatial attention based on either internal goals (endogenous or goal-driven) or distinctive sensory stimuli (exogenous or stimulus-driven) (Corbetta and Shulman, 2002; Corbetta et al., 2008). This study demonstrated that reorienting, as compared to maintaining, attention induced a more sustained desynchronization in the low-β band that was selectively observed in the DAN, especially in the FEF. Crucially, this prolonged desynchronization was positively associated with task performance, in terms of both accuracy and speed of target discrimination. Control analyses ruled out an explanation of these modulations in terms of motor preparation (Pfurtscheller, 1981; Crone et al., 1998; Wang, 2010). Moreover, the anatomical specificity (see the whole-brain analysis) and the sustained and relatively late peak latency (~450 ms) do not support an interpretation of this effect as a general "arousal signal" to shift cues (Wrobel, 2000). Our interpretation is that the prolonged β band desynchronization observed in the DAN, especially in FEF, reflects the re-routing of information processing from one hemisphere/visual system to the other, and the maintenance of top-down preparation of visual representations before the target arrives, consistently with multiple fMRI studies (e.g. Sylvester et al. 2007). The need for specific shift-related control signals (reviewed in Corbetta and Shulman 2002, Corbetta et al. 2008) explains the prolonged modulation for shift as compared to stay cues. Our results extend previous EEG/MEG studies that have also revealed beta (and alpha) desynchronization in the preparatory period following a spatial *orienting* cue (e.g.Siegel et al., 2008). Moreover, the relevance of the temporal dynamics of β oscillations for reorienting performance broadens our knowledge on the role of this

rhythmical activity for performance in visual tasks (Gross et al., 2004; Donner et al., 2007; Chanes et al., 2013).

Within the DAN, a prominent role in reorienting seems to be played by the prefrontal regions. Our results complement previous evidence about the causal role of the FEF in shifts of attention (Grosbras and Paus, 2002; Duecker et al., 2013; Heinen et al., 2017). For instance, a recent TMS study employing a visuospatial attention task showed that temporary perturbation of neural activity in right FEF impairs target detection specifically after shift cues (Heinen et al., 2017). Our results are also consistent with the results of directional analyses supporting a prominent top-down role of FEF on posterior parietal and occipital visual regions obtained in fMRI (Bressler et al., 2008; Spadone et al., 2015); MEG (Popov et al., 2017), and micro-stimulation studies (Moore and Armstrong, 2003).

In summary, several properties of the β band modulation observed in the DAN, such as its spatial distribution, temporal profile, and relationship with behavioral performance are compatible with its involvement in the control of attentional reorienting. The long-lasting β band suppression might reflect the influence of the high-order areas over the visual periphery, acting as to pre-establish novel (sensory) representations before the target arrives. These representations might be on the top of the rerouting of the information across hemispheres, with the β band playing a crucial role in the long-distance signaling along feedback pathways (Wang, 2010).

4.2. θ-band early reset modulation

Previous fMRI studies have related the reorienting response to the recruitment of the VAN, DAN, and CON. Visuospatial attention fMRI studies found a specific response in both VAN (right temporo-parietal, right inferior frontal), and DAN (IPS, FEF) regions when subjects reoriented attention to a novel location (reviewed in Corbetta and Shulman 2002; see also Shulman et al. 2009 on a similar task). However, later studies showed the same regions/networks to respond also to the onset/offset of task sets (e.g., Dosenbach et al. 2008). This led to the more general hypothesis that the reorienting modulation in these regions reflects 'interrupt' or 'network reset' activity signaling the presence of novel behaviorally relevant stimuli that require a change in task set (Corbetta et al., 2008). Importantly, EEG studies and subsequent ECoG studies demonstrated that this signal is not 'early' but reflects a post-detection adjustment, akin to a P300 response (Corbetta et al., 2008; Daitch et al., 2013).

In this study, we show a transient θ ERS modulation with a latency of about 300 ms stronger for reorienting (shift>stay) involving VAN, FPN, CO, but also DAN and VIS networks (Corbetta et al., 2008; Dosenbach et al., 2008). Several properties of the θ rhythm modulation (i.e. transient, short-latency, amplitude modulation, independence from cue side) are consistent with an alert/reset signal that helps in the reconfiguration of task networks, as proposed by previous fMRI work (Corbetta et al., 2008).

Notably, theta ERS modulations have been also observed in recent MEG (Proskovec et al., 2018) and ECoG (Daitch et al., 2013) studies that examined reorienting responses using a Posner-like paradigm. However, our task is unique as it allows a precise isolation of reorienting processes (shift vs. stay cues) independently of visual stimulation, target detection, response preparation/execution. Also, our combined fMRI-driven ROI and whole-brain analysis allow for a complete description of the anatomy of this modulation as compared to previous studies.

4.3. α and high-β/γ bands visual occipital modulations

In agreement with a vast EEG/MEG literature on the roles of alpha and gamma rhythms in visual processing (Jensen and Mazaheri, 2010; Bastos et al., 2015; Gregoriou et al., 2015; Jensen et al., 2015), shift cues further induced an expected contralateral modulation of both α (greater ERD for contra vs. ipsilateral shift cues) and low-γ (longer ERS for contra vs. ipsilateral shift cues) specifically in the visual regions (see the whole-brain analysis for spatial specificity). The pre-stimulus suppression of α activity in visual regions is consistent with the result of previous EEG/MEG studies associating decrements/increments of α power to enhanced/inhibited information processing, respectively, during orienting of attention (Thut et al., 2006; Siegel et al., 2008; Capotosto et al., 2009; Mazaheri et al., 2014; D'Andrea et al., 2019), and other cognitive tasks (Capotosto et al., 2017; Spadone et al., 2017, 2020). A shift-related effect on α oscillations has also been found in previous studies looking at target-induced reorienting (Sauseng et al., 2005; Proskovec et al., 2018).

The contralateral selective modulation of the α ERD amplitude throughout the cue-target period is consistent with a preparatory modulation of sensory processing in the visual cortex in the anticipation of the target, possibly reflecting stronger inhibition of previously attended visual stimuli after shift cues.

In contrast, the observed modulation of ERS duration in the γ band occurred late in the visual cortex, supporting its role in the modulation of sensory processing at the newly attended location, through the amplification of feedforward signals, following an attention shift (Fries, 2009; Gregoriou et al., 2009). The continuous sensory stimulation characterizing the present paradigm likely explains why this modulation was observed before the target presentation, consistent with a previous report of γ synchronizations in monkey visual cortex during pre-stimulus attention selection (Fries et al., 2001).

4.4. A cascade of neurophysiological mechanisms involved in attentional reorienting

Our work shows, for the first time in the same experiment, a cascade of frequency-specific modulations that unfolds over time, reflecting different aspects of the reorienting response. As shown in Fig. 7, a theta band synchronization of task-relevant networks (DAN, VIS), and additional control networks (VAN, CO, FPN) reflects an early alert/reset signal. Concurrently, the DAN implements the re-routing of relevant information across hemispheres (visual fields) through a sustained desynchronization of the low-β band, especially in FEF. In the visual system, the reorienting response manifests locally with well-known alpha desynchronization stronger contralaterally to shift cues. Based on current models (e.g. Jensen and Mazaheri 2010) this modulation reflects the inhibition of previously attended visual stimuli. Finally, preparatory processes indexed by γ-band synchronization may reflect anticipatory boosting of stimulus processing at the new location, which lasts longer for shift than stay cues.

Finally, to complement the results presented in this work, future investigations could analyze the functional interaction between the task-relevant regions of the DAN and VIS during attentional reorienting.

Credit authorship contribution statement

Sara Spadone: Methodology, Software, Formal analysis, Investigation, Writing – original draft. **Viviana Betti:** Investigation, Writing – review & editing. **Carlo Sestieri:** Formal analysis, Investigation, Writing – review & editing. **Vittorio Pizzella:** Writing – review & editing. **Maurizio Corbetta:** Conceptualization, Writing – review & editing, Supervision. **Stefania Della Penna:** Conceptualization, Methodology, Writing – review & editing, Supervision.

Acknowledgments

We warmly thank Prof. Gian Luca Romani for his scientific advice.

MC was supported by a Strategic Grant from the University of Padova, FLAG-ERA JTC (Brain-Synch HIT). SS was supported by a fellowship from BIAL foundation (Grant No #159–2016 to CS). VB has received funding from the European Research Council (ERC) under the European Union's s Horizon 2020 Research and Innovation program (Grant

Agreement No. 759651). This work was supported by the "Departments of Excellence 2018–2022″ initiative of the Italian Ministry of Education, University and Research for the Department of Neuroscience, Imaging and Clinical Sciences (DNISC) of the University of Chieti-Pescara, and for the Department of Neuroscience University of Padua.

Data/code availability statement

The empirical data used for this paper will be available in the public repository “Mendeley Data” (https://data.mendeley.com/) before the eventual final submission. The codes used for this paper are available upon request from the corresponding author.

Supplementary materials

Supplementary material associated with this article can be found, in the online version, at doi:10.1016/j.neuroimage.2021.118616.

References

Baldassarre, A., Ramsey, L., Hacker, C.L., Callejas, A., Astafiev, S.V., Metcalf, N.V., Zinn, K., Rengachary, J., Snyder, A.Z., Carter, A.R., Shulman, G.L., Corbetta, M., 2014. Large-scale changes in network interactions as a physiological signature of spatial neglect. Brain 137, 3267–3283.

Bastos, A.M., Vezoli, J., Bosman, C.A., Schoffelen, J.M., Oostenveld, R., Dowdall, J.R., De Weerd, P., Kennedy, H., Fries, P., 2015. Visual areas exert feedforward and feedback influences through distinct frequency channels. Neuron 85, 390–401.

Bauer, M., Stenner, M.P., Friston, K.J., Dolan, R.J., 2014. Attentional modulation of alpha/beta and gamma oscillations reflect functionally distinct processes. J. Neurosci. 34, 16117–16125.

Bressler, S.L., Tang, W., Sylvester, C.M., Shulman, G.L., Corbetta, M., 2008. Top-down control of human visual cortex by frontal and parietal cortex in anticipatory visual spatial attention. J. Neurosci. 28, 10056–10061.

Bulling, A., Ward, J.A., Gellersen, H., Troster, G., 2011. Eye movement analysis for activity recognition using electrooculography. IEEE Trans. Pattern Anal. Mach. Intell. 33, 741–753.

Buschman, T.J., Miller, E.K., 2007. Top-down versus bottom-up control of attention in the prefrontal and posterior parietal cortices. Science 315, 1860–1862.

Capotosto, P., Babiloni, C., Romani, G.L., Corbetta, M., 2009. Frontoparietal cortex controls spatial attention through modulation of anticipatory alpha rhythms. J. Neurosci. 29, 5863–5872.

Capotosto, P., Baldassarre, A., Sestieri, C., Spadone, S., Romani, G.L., Corbetta, M., 2017. Task and regions specific top-down modulation of alpha rhythms in parietal cortex. Cereb. Cortex 27, 4815–4822.

Capotosto, P., Spadone, S., Tosoni, A., Sestieri, C., Romani, G.L., Della Penna, S., Corbetta, M., 2015. Dynamics of EEG rhythms support distinct visual selection mechanisms in parietal cortex: a simultaneous transcranial magnetic stimulation and EEG study. J. Neurosci. 35, 721–730.

Capotosto, P., Tosoni, A., Spadone, S., Sestieri, C., Perrucci, M.G., Romani, G.L., Della Penna, S., Corbetta, M., 2013. Anatomical segregation of visual selection mechanisms in human parietal cortex. J. Neurosci. 33, 6225–6229.

Chanes, L., Quentin, R., Tallon-Baudry, C., Valero-Cabre, A., 2013. Causal frequency-specific contributions of frontal spatiotemporal patterns induced by non-invasive neurostimulation to human visual performance. J. Neurosci. 33, 5000–5005.

Corbetta, M., 1998. Frontoparietal cortical networks for directing attention and the eye to visual locations: identical, independent, or overlapping neural systems? Proc. Natl. Acad. Sci. U.S.A. 95, 831–838.

Corbetta, M., Shulman, G.L., 2002. Control of goal-directed and stimulus-driven attention in the brain. Nat. Rev. Neurosci. 3, 201–215.

Corbetta, M., Kincade, J.M., Shulman, G.L., 2002. Neural systems for visual orienting and their relationships to spatial working memory. J. Cogn. Neurosci. 14, 508–523.

Corbetta, M., Patel, G., Shulman, G.L., 2008. The reorienting system of the human brain: from environment to theory of mind. Neuron 58, 306–324.

Crone, N.E., Miglioretti, D.L., Gordon, B., Sieracki, J.M., Wilson, M.T., Uematsu, S., Lesser, R.P., 1998. Functional mapping of human sensorimotor cortex with electrocorticographic spectral analysis. I. Alpha and beta event-related desynchronization. Brain 121 (Pt 12), 2271–2299.

D’Andrea, A., Chella, F., Marshall, T.R., Pizzella, V., Romani, G.L., Jensen, O., Marzetti, L., 2019. Alpha and alpha-beta phase synchronization mediate the recruitment of the visuospatial attention network through the superior longitudinal fasciculus. Neuroimage 188, 722–732.

Daitch, A.L., Sharma, M., Roland, J.L., Astafiev, S.V., Bundy, D.T., Gaona, C.M., Snyder, A.Z., Shulman, G.L., Leuthardt, E.C., Corbetta, M., 2013. Frequency-specific mechanism links human brain networks for spatial attention. Proc. Natl. Acad. Sci. U.S.A. 110, 19585–19590.

Della Penna, S., Torquati, K., Pizzella, V., Babiloni, C., Franciotti, R., Rossini, P.M., Romani, G.L., 2004. Temporal dynamics of alpha and beta rhythms in human SI and SII after galvanic median nerve stimulation. A MEG study. Neuroimage 22, 1438–1446.

Della Penna, S., Del Gratta, C., Granata, C., Pasquarelli, A., Pizzella, V., Rossi, R., Russo, M., Torquatiand, K., Erné, S.N., 2000. Biomagnetic systems for clinical use. Philos. Magn. B Phys. Condens. Matter Stat. Mech. Electron. Opt. Magn. Prop. 80, 937–948.

Donner, T.H., Siegel, M., Oostenveld, R., Fries, P., Bauer, M., Engel, A.K., 2007. Population activity in the human dorsal pathway predicts the accuracy of visual motion detection. J. Neurophysiol. 98, 345–359.

Dosenbach, N.U., Fair, D.A., Cohen, A.L., Schlaggar, B.L., Petersen, S.E., 2008. A dual-networks architecture of top-down control. Trends Cogn. Sci. (Regul. Ed.) 12, 99–105.

Dosenbach, N.U., Fair, D.A., Miezin, F.M., Cohen, A.L., Wenger, K.K., Dosenbach, R.A., Fox, M.D., Snyder, A.Z., Vincent, J.L., Raichle, M.E., Schlaggar, B.L., Petersen, S.E., 2007. Distinct brain networks for adaptive and stable task control in humans. Proc. Natl. Acad. Sci. U.S.A. 104, 11073–11078.

Duecker, F., Formisano, E., Sack, A.T., 2013. Hemispheric differences in the voluntary control of spatial attention: direct evidence for a right-hemispheric dominance within frontal cortex. J. Cogn. Neurosci. 25, 1332–1342.

Favaretto, C., Spadone, S., Sestieri, C., Betti, V., Cenedese, A., Della Penna, S., Corbetta, M., 2021. Multi-band MEG signatures of BOLD connectivity reorganization during visuospatial attention. Neuroimage 230, 117781.

Fiebelkorn, I.C., Pinsk, M.A., Kastner, S., 2018. A dynamic interplay within the frontoparietal network underlies rhythmic spatial attention. Neuron 99, 842–853 e848.

Fries, P., 2009. Neuronal gamma-band synchronization as a fundamental process in cortical computation. Annu. Rev. Neurosci. 32, 209–224.

Fries, P., Reynolds, J.H., Rorie, A.E., Desimone, R., 2001. Modulation of oscillatory neuronal synchronization by selective visual attention. Science 291, 1560–1563.

Gregoriou, G.G., Paneri, S., Sapountzis, P., 2015. Oscillatory synchrony as a mechanism of attentional processing. Brain Res. 1626, 165–182.

Gregoriou, G.G., Gotts, S.J., Zhou, H., Desimone, R., 2009. High-frequency, long-range coupling between prefrontal and visual cortex during attention. Science 324, 1207–1210.

Grosbras, M.H., Paus, T., 2002. Transcranial magnetic stimulation of the human frontal eye field: effects on visual perception and attention. J. Cogn. Neurosci. 14, 1109–1120.

Gross, J., Schmitz, F., Schnitzler, I., Kessler, K., Shapiro, K., Hommel, B., Schnitzler, A., 2004. Modulation of long-range neural synchrony reflects temporal limitations of visual attention in humans. Proc. Natl. Acad. Sci. U.S.A. 101, 13050–13055.

Heinen, K., Feredoes, E., Ruff, C.C., Driver, J., 2017. Functional connectivity between prefrontal and parietal cortex drives visuo-spatial attention shifts. Neuropsychologia 99, 81–91.

Hopfinger, J.B., Buonocore, M.H., Mangun, G.R., 2000. The neural mechanisms of top–down attentional control. Nat. Neurosci. 3, 284–291.

Jensen, O., Mazaheri, A., 2010. Shaping functional architecture by oscillatory alpha activity: gating by inhibition. Front. Hum. Neurosci. 4, 186.

Jensen, O., Hari, R., Kaila, K., 2002. Visually evoked gamma responses in the human brain are enhanced during voluntary hyperventilation. Neuroimage 15, 575–586.

Jensen, O., Bonnefond, M., Marshall, T.R., Tiesinga, P., 2015. Oscillatory mechanisms of feedforward and feedback visual processing. Trends Neurosci. 38, 192–194.

Kastner, S., Pinsk, M.A., De Weerd, P., Desimone, R., Ungerleider, L.G., 1999. Increased activity in human visual cortex during directed attention in the absence of visual stimulation. Neuron 22, 751–761.

Larson-Prior, L.J., Oostenveld, R., Della Penna, S., Michalareas, G., Prior, F., Babajani-Feremi, A., Schoffelen, J.M., Marzetti, L., de Pasquale, F., Di Pompeo, F., Stout, J., Woolrich, M., Luo, Q., Bucholz, R., Fries, P., Pizzella, V., Romani, G.L., Corbetta, M., Snyder, A.Z., 2013. Adding dynamics to the human connectome project with MEG. Neuroimage 80, 190–201.

Mantini, D., Della Penna, S., Marzetti, L., de Pasquale, F., Pizzella, V., Corbetta, M., Romani, G.L., 2011. A signal-processing pipeline for magnetoencephalography resting-state networks. Brain Connect. 1, 49–59.

Mazaheri, A., van Schouwenburg, M.R., Dimitrijevic, A., Denys, D., Cools, R., Jensen, O., 2014. Region-specific modulations in oscillatory alpha activity serve to facilitate processing in the visual and auditory modalities. Neuroimage 87, 356–362.

Meehan, T.P., Bressler, S.L., Tang, W., Astafiev, S.V., Sylvester, C.M., Shulman, G.L., Corbetta, M., 2017. Top-down cortical interactions in visuospatial attention. Brain Struct. Funct. 222, 3127–3145.

Moore, T., Armstrong, K.M., 2003. Selective gating of visual signals by microstimulation of frontal cortex. Nature 421, 370–373.

Neuper, C., Pfurtscheller, G., 2001. Event-related dynamics of cortical rhythms: frequency-specific features and functional correlates. Int. J. Psychophysiol. 43, 41–58.

Pfurtscheller, G., 1981. Central beta rhythm during sensorimotor activities in man. Electroencephalogr. Clin. Neurophysiol. 51, 253–264.

Pizzella, V., Della Penna, S., Del Gratta, C., Romani, G.L., 2001. SQUID systems for biomagnetic imaging. Supercond. Sci. Technol. 14, R79–R114.

Popov, T., Kastner, S., Jensen, O., 2017. Fef-controlled alpha delay activity precedes stimulus-induced gamma-band activity in visual cortex. J. Neurosci. 37, 4117–4127.

Proskovec, A.L., Heinrichs-Graham, E., Wiesman, A.I., McDermott, T.J., Wilson, T.W., 2018. Oscillatory dynamics in the dorsal and ventral attention networks during the reorienting of attention. Hum. Brain Mapp. 39, 2177–2190.

Rizzolatti, G., Riggio, L., Dascola, I., Umilta, C., 1987. Reorienting attention across the horizontal and vertical meridians: evidence in favor of a premotor theory of attention. Neuropsychologia 25, 31–40.

Sauseng, P., Klimesch, W., Stadler, W., Schabus, M., Doppelmayr, M., Hanslmayr, S., Gruber, W.R., Birbaumer, N., 2005. A shift of visual spatial attention is selectively associated with human EEG alpha activity. Eur. J. Neurosci. 22, 2917–2926.

Sebastiani, V., de Pasquale, F., Costantini, M., Mantini, D., Pizzella, V., Romani, G.L., Della Penna, S., 2014. Being an agent or an observer: different spectral dynamics revealed by MEG. Neuroimage 102 (Pt 2), 717–728.

Seeley, W.W., Menon, V., Schatzberg, A.F., Keller, J., Glover, G.H., Kenna, H., Reiss, A.L., Greicius, M.D., 2007. Dissociable intrinsic connectivity networks for salience processing and executive control. J. Neurosci. 27, 2349–2356.

Shulman, G.L., Pope, D.L., Astafiev, S.V., McAvoy, M.P., Snyder, A.Z., Corbetta, M., 2010. Right hemisphere dominance during spatial selective attention and target detection occurs outside the dorsal frontoparietal network. J. Neurosci. 30, 3640–3651.

Shulman, G.L., Astafiev, S.V., Franke, D., Pope, D.L., Snyder, A.Z., McAvoy, M.P., Corbetta, M., 2009. Interaction of stimulus-driven reorienting and expectation in ventral and dorsal frontoparietal and basal ganglia-cortical networks. J. Neurosci. 29, 4392–4407.

Siegel, M., Donner, T.H., Oostenveld, R., Fries, P., Engel, A.K., 2008. Neuronal synchronization along the dorsal visual pathway reflects the focus of spatial attention. Neuron 60, 709–719.

Spadone, S., de Pasquale, F., Mantini, D., Della Penna, S., 2012. A K-means multivariate approach for clustering independent components from magnetoencephalographic data. Neuroimage 62, 1912–1923.

Spadone, S., Sestieri, C., Baldassarre, A., Capotosto, P., 2017. Temporal dynamics of TMS interference over preparatory alpha activity during semantic decisions. Sci. Rep. 7, 2372.

Spadone, S., Croce, P., Zappasodi, F., Capotosto, P., 2020. Pre-stimulus EEG microstates correlate with anticipatory alpha desynchronization. Front. Hum. Neurosci. 14, 182.

Spadone, S., Della Penna, S., Sestieri, C., Betti, V., Tosoni, A., Perrucci, M.G., Romani, G.L., Corbetta, M., 2015. Dynamic reorganization of human resting-state networks during visuospatial attention. Proc. Natl. Acad. Sci. U.S.A. 112, 8112–8117.

Sylvester, C.M., Shulman, G.L., Jack, A.I., Corbetta, M., 2007. Asymmetry of anticipatory activity in visual cortex predicts the locus of attention and perception. J. Neurosci. 27, 14424–14433.

Thut, G., Nietzel, A., Brandt, S.A., Pascual-Leone, A., 2006. Alpha-band electroencephalographic activity over occipital cortex indexes visuospatial attention bias and predicts visual target detection. J. Neurosci. 26, 9494–9502.

Torquati, K., Pizzella, V., Babiloni, C., Del Gratta, C., Della Penna, S., Ferretti, A., Franciotti, R., Rossini, P.M., Romani, G.L., 2005. Nociceptive and non-nociceptive sub-regions in the human secondary somatosensory cortex: an MEG study using fMRI constraints. Neuroimage 26, 48–56.

Wang, X.J., 2010. Neurophysiological and computational principles of cortical rhythms in cognition. Physiol. Rev. 90, 1195–1268.

Wrobel, A., 2000. Beta activity: a carrier for visual attention. Acta Neurobiol. Exp. (Wars) 60, 247–260.

Xia, M., Wang, J., He, Y., 2013. BrainNet Viewer: a network visualization tool for human brain connectomics. PLoS ONE 8, e68910.